DOI: 10.1021/ic902394m

Inorganic Chemistry
Article

Synthesis, Crystal Structures, and Physical Properties of the Novel $Ca_xR_{17-x}Mo_{19}O_{46}$ ($4 \leq x \leq 7$; R = Ce, Pr, Sm, and Gd) Compounds Containing Centered Mo_{19} ν_2-Octahedral Clusters

N. Barrier,[†] P. Gall,[‡] T. Guizouarn,[‡] and P. Gougeon*[,‡]

[†]*Laboratoire CRISMAT, UMR CNRS 6508, 6 Boulevard Maréchal Juin, 14050 Caen Cedex 4, France, and* [‡]*Sciences Chimiques de Rennes, UMR CNRS 6226, INSA, Université de Rennes 1, Avenue du Général Leclerc, 35042 Rennes, France*

Received December 3, 2009

The novel quaternary reduced molybdenum oxides $Ca_xR_{17-x}Mo_{19}O_{46}$ ($4 \leq x \leq 7$; R = Ce, Pr, Sm, and Gd) have been synthesized by a solid-state reaction at 1400 °C for 48 h in sealed molybdenum crucibles. The crystal structure was determined on a single crystal of $Ca_{5.24}R_{11.76}Mo_{19}O_{46}$ by X-ray diffraction. This compound crystallizes in the monoclinic space group *C*2/*m*: *a* = 19.5192(4) Å, *b* = 11.1244(3) Å, *c* = 13.2589(5) Å, β = 132.055(1)°, *V* = 2137.7(1) Å^3, *Z* = 2. Refinements yield R1(F^2) = 0.0388 and wR2(F^2) = 0.0792 for 5667 unique reflections. The structure is built up from alternating slabs made up of Mo forming centered Mo_{19} ν_2-octahedral clusters, Ca, Pr, and O atoms and slabs containing only Ca, Pr, and O atoms. The Mo_{19} cluster, in which the Mo−Mo distances range from 2.7274(4) to 2.7940(7) Å, results from a three-dimensional condensation of six Mo_6 octahedra. The Ca^{2+} and Pr^{3+} cations occupy seven crystallographically independent sites with coordination numbers in the O atoms varying from 6 to 8. Magnetic susceptibility measurements made on the $Ca_xPr_{17-x}Mo_{19}O_{46}$ (x = 4−7) compounds confirm the presence of Pr^{3+} cations, and no magnetic ordering was observed down to 4.2 K. Electrical resistivity measurements on a single crystal of $Ca_{\sim 5}Pr_{\sim 12}Mo_{19}O_{46}$ show a semiconducting behavior.

1. Introduction

The structural chemistry of compounds containing reduced molybdenum has grown tremendously over the last 2 decades so that 22 different types of discrete molybdenum clusters, the nuclearities of which range from 3 to 36, are known to date. Clusters with nuclearities higher than 8 result generally from the one-dimensional condensation of Mo_6 clusters via opposite face- or edge-sharing depending on the ligand environment. The former process is observed when the Mo_6 clusters are face-bridged by the ligands (S, Se, and Te) and is exemplified, in particular, by the series of compounds $M_{n-2}Mo_{3n}X_{3n+2}$ (M = Rb, and Cs; X = S, Se, or Te; n = 3−8, 10, and 12) containing Mo_{3n} clusters.[1−7] The final stage of this face-sharing condensation is the infinite $|Mo_{6/2}|^1_\infty$ chain found in the quasi-one-dimensional compounds $M_2Mo_6X_6$ (M = Na, K, Rb, and Cs; X = S, Se, or Te)[8] and $AgMo_6Te_6$.[9] The edge-sharing condensation of Mo_6 octahedra is observed in reduced molybdenum oxides, where the Mo_6 clusters are edge-bridged by the O atoms. This process leads to Mo_{4n+2} oligomers that are observed, for example, in the series $M_{n-x}Mo_{4n+2}O_{6n+4}$ (n = 2−5).[10−21] The ultimate

*To whom correspondence should be addressed. E-mail: Patrick.Gougeon@univ-rennes1.fr. Fax: int. code +2 23 23 67 99.

(1) Gougeon, P.; Padiou, J.; Le Marouille, J.-Y.; Potel, M.; Sergent, M. *J. Solid State Chem.* **1984**, *51*, 218.
(2) Gougeon, P.; Potel, M.; Padiou, J.; Sergent, M. *Mater. Res. Bull.* **1987**, *22*, 1087.
(3) Gougeon, P.; Potel, M.; Sergent, M. *Acta Crystallogr.* **1989**, *C45*, 182.
(4) Gougeon, P.; Potel, M.; Sergent, M. *Acta Crystallogr.* **1989**, *C45*, 1413.
(5) Gougeon, P.; Potel, M.; Padiou, J.; Sergent, M. *Mater. Res. Bull.* **1988**, *23*, 453.
(6) Gougeon, P.; Potel, M.; Sergent, M. *Acta Crystallogr.* **1990**, *C46*, 2284.
(7) Picard, S.; Gougeon, P.; Potel, M. *Acta Crystallogr.* **1997**, *C53*, 1519.
(8) Gougeon, P. Thesis, Université de Rennes 1, Rennes, France, **1984**.
(9) Gougeon, P.; Potel, M.; Padiou, J.; Sergent, M. *J. Solid State Chem.* **1987**, *68*, 137.
(10) Hibble, S. J.; Cheetham, A. K.; Bogle, A. R. L.; Wakerley, H. R.; Cox, D. E. *J. Am. Chem. Soc.* **1988**, *110*, 3295.
(11) Dronskowski, R.; Simon, A. *Angew. Chem., Int. Ed. Engl.* **1989**, *28*, 758.
(12) Gougeon, P.; Potel, M.; Sergent, M. *Acta Crystallogr.* **1990**, *C46*, 1188.
(13) Gougeon, P.; Gall, P.; Sergent, M. *Acta Crystallogr.* **1991**, *C47*, 421.
(14) Dronskowski, R.; Simon, A.; Mertin, W. *Z. Anorg. Allg. Chem.* **1991**, *602*, 49.
(15) Gall, P.; Gougeon, P. *Acta Crystallogr.* **1994**, *C50*, 7.
(16) Gall, P.; Gougeon, P. *Acta Crystallogr.* **1994**, *C50*, 1183.
(17) Dronskowski, R.; Simon, A. *Acta Chem. Scand.* **1991**, *45*, 850.
(18) Schimek, G. L.; Chen, S. C.; Mc Carley, R. E. *Inorg. Chem.* **1995**, *34*, 6130.
(19) Schimek, G. L.; Nagaki, D. A.; Mc Carley, R. E. *Inorg. Chem.* **1994**, *33*, 1259.
(20) Dronskowski, R.; Mattausch, H. J.; Simon, A. *Z. Anorg. Allg. Chem.* **1993**, *619*, 1397.
(21) Schimek, G. L.; Mc Carley, R. E. *J. Solid State Chem.* **1994**, *113*, 345.

 Published on Web 01/25/2010

Table 1. Unit-Cell Parameters for the $Ca_{\sim 5}R_{\sim 12}Mo_{19}O_{46}$ (R = Ce, Pr, Sm, and Gd) Compounds

compound	*a* (Å)	*b* (Å)	*c* (Å)	*β* (deg)	*V* (Å^3)
$Ca_{5.38}Ce_{11.62}Mo_{19}O_{46}$	19.5751(5)	11.1614(3)	13.2812(4)	132.049(1)	2154.8(1)
$Ca_{5.24}Pr_{11.76}Mo_{19}O_{46}$	19.5192(4)	11.1244(3)	13.2589(5)	132.055(2)	2137.7(1)
$Ca_{4.99}Sm_{12.01}Mo_{19}O_{46}$	19.3703(3)	11.0386(2)	13.1768(2)	132.0661(9)	2091.61(6)
$Ca_{5.24}Gd_{11.76}Mo_{19}O_{46}$	19.2966(5)	10.9934(3)	13.1220(4)	132.011(1)	2068.3(1)

step of the edge-sharing-condensation process corresponds to the infinite $|Mo_2Mo_{4/2}|^1_\infty$ chain of trans-edge-sharing Mo_6 octahedra that was first observed in $NaMo_4O_6$.[22] More recently, two original high-nuclearity molybdenum clusters, i.e., Mo_{13} and Mo_{19}, were observed to be in coexistence with the common triangular Mo_3 and the planar Mo_7 clusters in the atypical compound $Pr_4Mo_9O_{18}$.[23] Contrary to the previous high-nuclearity molybdenum clusters, Mo_{13} and Mo_{19} result, for the first time in solid-state chemistry, from the bi- or tridimensional condensation of octahedral Mo_6 clusters, respectively. We present here the synthesis, crystal structure and magnetic susceptibility and resitivity measurements of the new series of compounds $Ca_{\sim 5}R_{\sim 12}Mo_{19}O_{46}$ (R = Ce, Pr, Sm, and Gd) containing only Mo_{19} clusters for the first time.

2. Experimental Section

2.1. Synthesis. Starting reagents were R_2O_3 (R = La, Sm, and Gd), CeO_2, or Pr_6O_{11} (Strem Chemicals, 99.999%), MoO_3 (Strem Chemicals, 99.9%), and Mo (Cimebocuze, 99.9%), all in powder form. The rare-earth oxide was prefired at 1000 °C before use, and the Mo powder was heated under a hydrogen flow at 1000 °C for 6 h. The stoichiometric mixture was pressed into a ca. 5 g pellet and loaded into a molybdenum crucible (depth 2.5 cm; diameter 1.5 cm), which was previously cleaned by heating at 1500 °C for 15 min under a dynamic vacuum of about 10^{-5} Torr and then sealed under a low argon pressure using an arc-welding system.

With the aim of modifying the physical properties of the compound $Pr_{16}Mo_{21}O_{56}$,[24] we tried to substitute a part of the Pr atoms by some Ca atoms. For that purpose, we realized synthesis in a sealed molybdenum crucible at 1600 °C during 48 h, from a mixture of powders of Pr_6O_{11}, $CaMoO_4$, MoO_3, and Mo with the nominal composition "$Ca_6Pr_{10}Mo_{21}O_{56}$". The powder X-ray diffraction pattern of the resulting product put in evidence the presence of two phases: Pr_3MoO_7[25] and another unknown phase for which some single crystals with the shape of small platelets were isolated. X-ray structural determination on one of these single crystals leads to the formula $Pr_{13.25}Mo_{19}O_{46}$ in the hypothesis of the absence of calcium. Quantitative microanalyses on the crystals thus obtained using a JEOL JSM-35 CF scanning electron microscope equipped with a Tracor energy-dispersive-type X-ray spectrometer showed that they contained some calcium and give a raw-approached formula $Ca_5Pr_{12}Mo_{19}O_{46}$. From this result, two syntheses were made at temperatures of 1400 and 1600 °C, with the nominal composition $Ca_5Pr_{12}Mo_{19}O_{46}$. At 1400 °C, we obtained a black powder only constituted by the new phase $Ca_5Pr_{12}Mo_{19}O_{46}$, and at 1600 °C, crystals of Pr_3MoO_7 and $Ca_5Pr_{12}Mo_{19}O_{46}$ were obtained. Afterward, the phases with La, Ce, Sm, and Gd isomorphous to $Ca_{\sim 5}Pr_{\sim 12}Mo_{19}O_{46}$ could be observed. However, we did not obtain a single-phase powder of the latter compounds and only single crystals of $Ca_{\sim 5}Ce_{\sim 12}Mo_{19}O_{46}$, $Ca_{\sim 5}Sm_{\sim 12}Mo_{19}O_{46}$, and $Ca_{\sim 5}Gd_{\sim 12}Mo_{19}O_{46}$ were obtained.

Table 1 collects the unit-cell parameters of compound $Ca_{\sim 5}R_{\sim 12}Mo_{19}O_{46}$ (R = Ce, Pr, Sm, and Gd). Attempts to synthesize isotructural compounds with Dy led to mixtures of the phases $CaMoO_4$ and Dy_2MoO_5, and the substitution of Ca for Sr ($Sr_5R_{12}Mo_{19}O_{46}$; R = La and Pr) yielded mixtures of $SrMoO_3$, La_3MoO_7, and Pr_3MoO_7. In the case of the Pr compound, reactions carried out with different ratios of Ca/Pr were also tested and led to single-phase products for compositions ranging from about $Ca_4Pr_{13}Mo_{19}O_{46}$ to $Ca_6Pr_{11}Mo_{19}O_{46}$.

2.2. Single-Crystal Structure Determination. A black crystal of dimensions $0.502 \times 0.420 \times 0.051$ mm^3 was selected for data collection. Intensity data were collected on a Nonius Kappa CCD diffractometer using graphite-monochromatized Mo Kα radiation (λ = 0.710 73 Å) at room temperature. The *COLLECT* program package[26] was used to establish the angular scan conditions (φ and ω scans) used in the data collection. The data set was processed using EvalCCD[27] for the integration procedure. An absorption correction (T_{min} = 0.5998; T_{max} = 0.7585) was applied using the *SORTAV* program.[28] The structure was solved by direct methods using *SIR97*[29] and subsequent difference Fourier syntheses in the space group *C*2/*m*. All structure refinements and Fourier syntheses were carried out using *SHELXL-97*.[30] Refinement of the occupancy factors of the Pr sites showed that the Pr1, Pr2, Pr3, Pr4, Pr5, and Pr6 sites are deficient. Because qualitative microanalyses using a JEOL JSM-35 CF scanning electron microscope equipped with a Tracor energy-dispersive-type X-ray spectrometer indicated the presence of Ca in the crystals with a ratio of Pr/Ca of about 2.1, we could expect that the deficiencies observed on the Pr sites result from the partial occupancy by Ca because in the final difference Fourier map we did not observe peaks compatible with the Ca positions. Consequently, an occupation of the deficient Pr sites simultaneously by Pr and Ca atoms was taking into account in the subsequent refinements. This is not surprising because the ionic radii of the Ca^{2+} and Pr^{3+} ions are very similar (1.12 and 1.14 Å in coordinence 8).[31] In the different mixed sites, the Pr and Ca atoms were constrained to have the same positional and anisotropic atomic displacement parameters and the sum of their site occupation factors was equal to 1 in further refinements. The positional and anisotropic displacement parameters for all atoms as well as the occupancy factors for the Pr and Ca atoms were refined to the values R1 = 0.0388 and wR2 = 0.0792 for 212 parameters and 5667 reflections with $I > 2\sigma(I)$, and the residual electron densities were +3.763 and −4.419 e Å^{-3}. A summary of the X-ray crystallographic and experimental data is presented in Table 2, and selected interatomic distances are reported in Table 3. Further details of the crystal structure investigation can be obtained from Fachinformationszentrum Karlsruhe, 76344 Eggenstein-Leopoldshafen, Germany (fax (49) 7247-808-666; e-mail crysdata@fiz.karlsruhe.de) on quoting the depository number CSD-421258.

(22) Torardi, C. C.; Mc Carley, R. E. *J. Am. Chem. Soc.* **1979**, *101*, 3963.
(23) Tortelier, J.; Gougeon, P. *Inorg. Chem.* **1998**, *37*(24), 6229.
(24) Gall, P.; Gautier, R.; Halet, J.-F.; Gougeon, P. *Inorg. Chem.* **1999**, *38* (20), 4455.
(25) Barrier, N.; Gougeon, P. *Acta Crystallogr.* **2003**, *E59*, i22.
(26) *COLLECT, data collection software*; Enraf-Nonius BV: Rotterdam, The Netherlands, 1999.
(27) Duisenberg, A. J. M. Reflections on Area Detectors. Ph.D. Thesis, University of Utrecht, Utrecht, The Netherlands, 1998.
(28) Blessing, R. H. *Acta Crystallogr.* **1995**, *A51*, 33–38.
(29) Altomare, A.; Burla, M. C.; Camalli, M.; Cascarano, G. L.; Giacovazzo, C.; Guagliardi, A.; Moliterni, A. G. G.; Polidori, G.; Spagna, R. *J. Appl. Crystallogr.* **1999**, *32*, 115.
(30) Sheldrick, G. M. *SHELXL97, Program for the Refinement of Crystal Structures*; University of Göttingen, Göttingen, Germany, 1997.
(31) Shannon, R. D.; Prewitt, C. T. *Acta Crystallogr.* **1969**, *B25*, 925.

Table 2. X-ray Crystallographic and Experimental Data for $Ca_{5.24}Pr_{11.76}Mo_{19}O_{46}$

formula	$Ca_{5.24(5)}Pr_{11.76(5)}Mo_{19}O_{46}$
fw (g mol^{-1})	4425.98
space group	$C2/m$
a (Å)	19.5192(5)
b (Å)	11.1244(3)
c (Å)	13.2549(4)
β (deg)	132.0549(14)
V (Å^3)	2137.7(1)
Z	2
ρ_{calc} (g cm^{-3})	6.876
T (°C)	20
λ (Å)	0.710 73 (Mo Kα)
μ (cm^{-1})	191.98
R1[a] [$I > 2\sigma(I)$]	0.0388
wR2[b] [$I > 2\sigma(I)$]	0.0792

[a] $R1 = \sum||F_o| - |F_c||/\sum|F_o|$. [b] $wR2 = \{\sum[w(F_o^2 - F_c^2)^2]/\sum[w(F_o^2)^2]\}^{1/2}$, $w = 1/[\sigma^2(F_o^2) + (0.0279P)^2 + 64.3224P]$, where $P = [\max(F_o^2,0) + 2F_c^2]/3$.

Table 3. Main Interatomic Distances (Å) in $Ca_{5.24}Pr_{11.76}Mo_{19}O_{46}$

Pr/Ca1−O14	2.253(5)	Pr/Ca4−O11	2.347(5)
Pr/Ca1−O11	2.255(5)	Pr/Ca4−O5 (×2)	2.370(4)
Pr/Ca1−O1 (×2)	2.514(4)	Pr/Ca4−O4	2.455(5)
Pr/Ca1−O1 (×2)	2.567(4)	Pr/Ca4−O3 (×2)	2.561(4)
Pr/Ca1−O2 (×2)	2.670(4)	Pr/Ca4−O6 (×2)	2.800(4)
Pr/Ca2−O5 (×2)	2.342(3)	Pr/Ca5−O12 (×4)	2.386(4)
Pr/Ca2−O14	2.360(5)	Pr/Ca5−O10 (×4)	2.800(4)
Pr/Ca2−O9 (×2)	2.457(4)		
Pr/Ca2−O7 (×2)	2.820(4)	Pr/Ca6−O12	2.243(4)
Pr/Ca2−O13	2.876(5)	Pr/Ca6−O11	2.258(3)
		Pr/Ca6−O6	2.353(4)
Pr/Ca3−O14	2.293(3)	Pr/Ca6−O3	2.384(3)
Pr/Ca3−O12	2.302(4)	Pr/Ca6−O8	2.692(4)
Pr/Ca3−O9	2.393(4)	Pr/Ca6−O6	2.765(4)
Pr/Ca3−O7	2.395(4)	Pr/Ca6−O2	2.977(4)
Pr/Ca3−O10	2.494(4)		
Pr/Ca3−O7	2.578(4)	Pr7−O4 (×2)	2.373(3)
Pr/Ca3−O13	2.785(4)	Pr7−O5 (×2)	2.429(4)
		Pr7−O12 (×2)	2.490(4)
Mo1−Mo5 (×2)	2.7341(6)	Mo4−Mo7	2.7423(6)
Mo1−Mo3 (×4)	2.7763(4)	Mo4−Mo6	2.7511(6)
Mo1−Mo2 (×2)	2.7935(6)	Mo4−Mo5	2.7643(5)
Mo1−Mo4 (×4)	2.7937(4)	Mo4−Mo3	2.7930(6)
		Mo4−Mo4	2.7938(8)
Mo2−Mo7	2.7275(4)		
Mo2−Mo7	2.7275(4)	Mo5−Mo7 (×2)	2.7533(4)
Mo2−Mo4 (×2)	2.7764(7)	Mo5−Mo3 (×2)	2.7591(5)
Mo2−Mo3 (×2)	2.7940(7)	Mo5−Mo4	2.7643(5)
Mo3−Mo6	2.7335(7)		
Mo3−Mo7	2.7346(6)	Mo6−Mo3	2.7335(7)
Mo3−Mo5	2.7591(5)	Mo6−Mo4 (x2)	2.7511(6)
Mo3−Mo3	2.7690(8)		
Mo3−Mo4	2.7930(6)	Mo7−Mo3	2.7346(6)
Mo2−O10 (×2)	2.047(4)	Mo5−O1 (×2)	2.074(4)
Mo2−O8	2.073(5)	Mo5−O2 (×2)	2.112(4)
Mo2−O13	2.106(5)		
		Mo6−O9 (×2)	2.010(4)
Mo3−O3	2.066(4)	Mo6−O3 (×2)	2.015(4)
Mo3−O6	2.071(4)	Mo6−O4	2.062(5)
Mo3−O2	2.095(4)		
Mo3−O8	2.102(4)		
		Mo7−O10	1.998(4)
Mo4−O9	2.075(4)	Mo7−O6	2.009(4)
Mo4−O2	2.077(4)	Mo7−O1	2.012(4)
Mo4−O13	2.095(4)	Mo7−O7	2.033(4)
Mo4−O7	2.099(4)	Mo7−O5	2.095(3)

2.3. Electrical Resistivity Measurements. The study of the temperature dependence of the electrical resistivity was carried out on a single crystal of $Ca_5Pr_{12}Mo_{19}O_{46}$ using a conventional alternating-current four-probe method with a current amplitude of 0.1 mA. Contacts were ultrasonically made with molten indium on the single crystal. The ohmic behavior and the invariance of the phase were checked during the different measurements at low and room temperature.

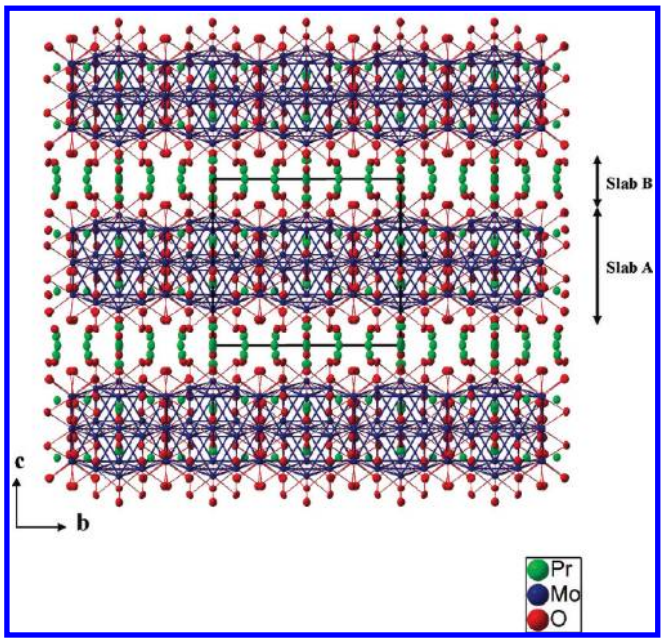

Figure 1. Perspective view of the crystal structure of $Ca_{5.24}Pr_{11.76}Mo_{19}O_{46}$ along the a axis.

2.4. Magnetic Susceptibility Measurements. Susceptibility data were collected on cold-pressed powder samples (ca. 100 mg) using a Quantum Design SQUID magnetometer between 4.2 and 400 K and at an applied field of 0.1 T.

3. Results and Discussion

3.1. Structure Description. A perspective view of the crystal structure of $Ca_{\sim 5}Pr_{\sim 12}Mo_{19}O_{46}$ along the a axis is represented in Figure 1. It shows that this structure can be viewed as a stacking along the c axis of two different slabs interconnected through O atoms. The first slab, labeled A, is made up of Mo forming Mo_{19} clusters, Ca, Pr, and O atoms, and the second slab, labeled B, contains only Ca, Pr, and O atoms.

In slab A, the presence of strong interactions between the Mo atoms leads to the formation of Mo_{19} clusters. The Mo_{19} cluster in these new compounds is similar to that encountered in $Pr_4Mo_9O_{18}$[23] and can be viewed as a result of the three-dimensional condensation of six Mo_6 octahedra around the same apex in such a way that every octahedron has four edges and five apexes in common with the neighboring octahedra, as depicted in Figure 2. The Mo_{19} cluster such as that presented on Figure 2 has crystallographic site symmetry C_{2h} instead of C_{3v} in $Pr_4Mo_9O_{18}$ and D_{3d} in $Mg_{4.5}Pr_{79.5}Mo_{126}O_{312}$[32] and is best considered as a centered ν_2-octahedron (alternatively, as a centered hexacapped cuboctahedron) of pseudo-O_h symmetry. The Mo−Mo distances in the Mo_{19} cluster only vary from 2.7341(6) to 2.7937(4) Å, which is comparable to those observed for the Mo_{19} clusters occurring in $Pr_4Mo_9O_{18}$ [2.7476(7)−2.805(2) Å] and

(32) Barrier, N.; Gall, P.; Gougeon, P. *J. Cluster Sci.* **2009**, *20*, 63.

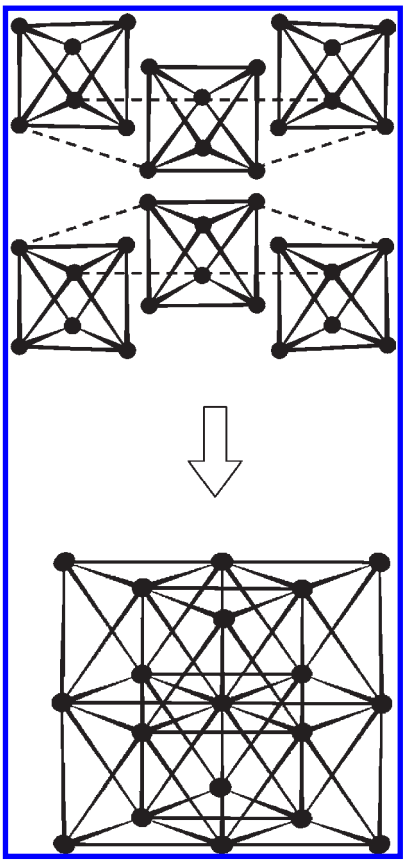

Figure 2. Condensation process for the Mo_{19} cluster.

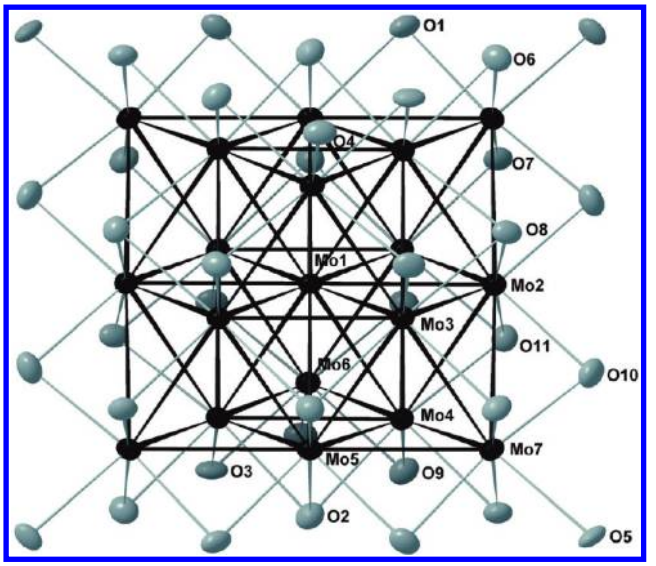

Figure 3. Mo_{19} cluster with its oxygen environment (97% probability ellipsoids).

$Mg_{4.5}Pr_{79.5}Mo_{126}O_{312}$ [2.7360(6)−2.8143(10) Å]. Compared to the other Mo clusters known in solid-state chemistry, one of the originalities of this cluster lies in the environment of the central atom Mo1, which is not linked to any O atom but to 12 other Mo atoms that form a distorted cuboctahedron. This type of cluster, in which a central atom is encapsulated, is much more observed frequently in organometallic chemistry with metals such as Pd, Rh, Re, Ru, Pt, or Os. The distances between the central atom Mo1 and its 12 neighbors are from 2.7341(6)

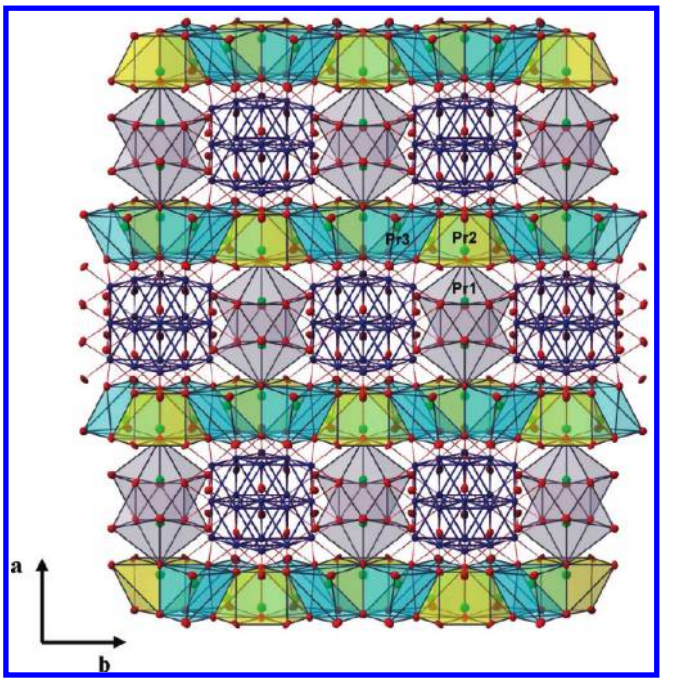

Figure 4. Polyhedral representation of slab A viewed along the *c* axis.

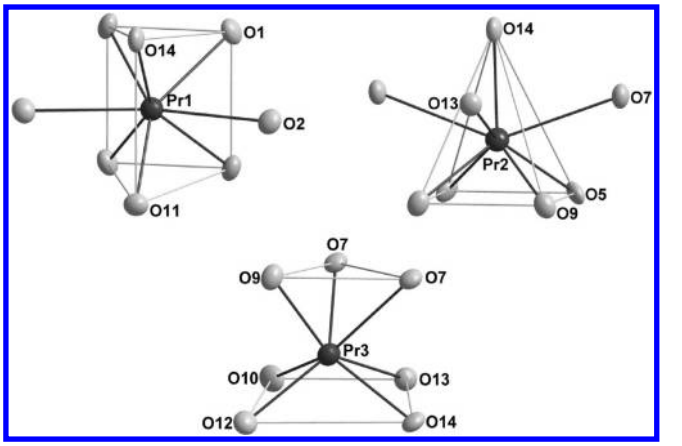

Figure 5. Oxygen environments for the Pr/Ca1, Pr/Ca2, and Pr/Ca3 atoms.

to 2.7937(4) Å, with a mean value of 2.778 Å. Other atoms, Mo2, Mo3, Mo4, and Mo5, are connected to seven atoms of Mo and to four atoms of O, while atoms Mo6 and Mo7 are connected only to four atoms of Mo and five atoms of O. All of these Mo and O atoms form the entity $Mo_{19}O_{38}$ (Figure 3). The atoms O1, O3, O6, O7, O9, and O10 bridge the Mo−Mo edges of the square bases of the Mo_6 octahedra, the atoms O2, O8, and O11 cap the triangular faces of the cluster Mo_{19}, and the atoms O4 and O5 are connected to the Mo in apical positions.

The projection of slab A is shown in Figure 4. In the latter slab, the shortest intercluster distance is 5.655(1) Å and the $Mo_{19}O_{38}$ units are only linked through O−Pr−O bridges. The three crystallographically independent Pr/Ca atoms in slab A present different environments (Figure 5). Pr1 has a bicapped trigonal-prismatic environment, with Pr1−O distances in the 2.253(5)−2.670(4) Å range. Pr2 is surrounded by eight O atoms forming a tricapped square-based pyramid. The Pr2−O bond distances lie between

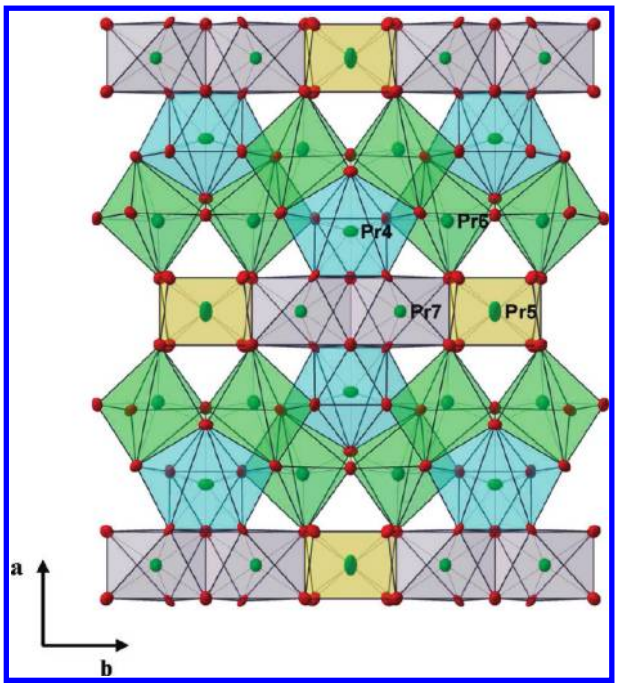

Figure 6. Polyhedral representation of slab B viewed along the *c* axis.

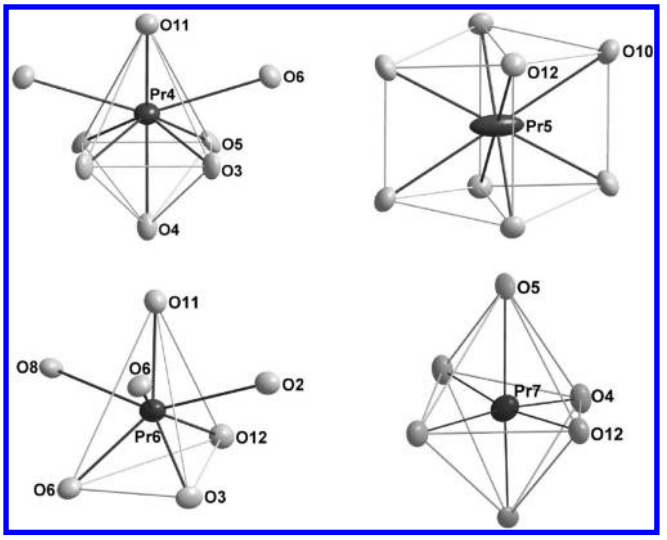

Figure 7. Oxygen environments for the Pr/Ca4, Pr/Ca5, Pr/Ca6, and Pr7 atoms.

2.342(3) and 2.876(5) Å. Finally, the $Pr3O_7$ polyhedron may be described as the stacking of a triangle formed by two O7 and one O9 atoms on a square of O10, O12, O13, and O14 atoms, with Pr−O distances comprised between 2.293(3) and 2.785(4) Å.

In slab B shown in Figure 6, we found the four other crystallographically independent Ca/Pr sites. The Ca/Pr4 and Ca/Pr5 atoms are eight-coordinate in oxygen but present different environments (Figure 7). Ca/Pr4 has a bicapped octahedral environment, and Ca/Pr5 is at the center of a distorted rhombus prism. The Ca/Pr4−O bond distances lie between 2.347(5) and 2.800(4) Å and the Ca/Pr5−O distances between 2.386(4) and 2.800(4) Å. The environment of the Ca/Pr6 atoms may be viewed as a distorted tricapped tetrahedron, with Ca/Pr6−O distances ranging from 2.243(4) to 2.977(4) Å. Finally, the

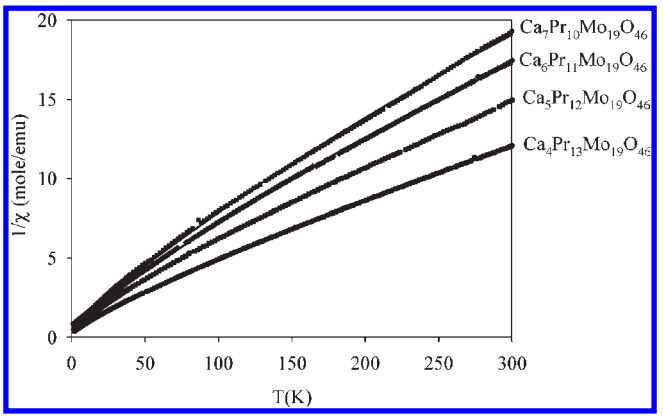

Figure 8. Reciprocal susceptibilities of $Ca_xPr_{17-x}Mo_{19}O_{46}$ (x = 4−7) as a function of the temperature. Data were taken under an applied field of 0.5 T. The solid lines represent a fit to the Curie−Weiss law in the range of 4.2−300 K.

Pr7 atom shows a distorted octahedral environment of O atoms, with Pr7−O distances varying between 2.373(3) and 2.490(4) Å.

3.2. Bond-Length Bond-Strength Formula. The estimation of the oxidation states of Mo and, consequently, of the number of electrons per Mo_{19} cluster could be performed on this compound using the empirical bond length−bond strength relationship developed by Brown and Wu[33] for Mo−O bonds:

$$s(\mathrm{Mo-O}) = [d(\mathrm{Mo-O})/1.882]^{-6}$$

In the above formula, s(Mo−O) is the bond strength in valence units, d(Mo−O) is the observed Mo−O bond distance in Ångström, 1.882 Å corresponds to a Mo−O single-bond distance, and the exponential parameter −6 is characteristic of the Mo atom. Thus, the sum of the Mo−O bond strengths s (in valence units) about a particular Mo atom is equal to the oxidation state of that Mo atom. For the six crystallographically independent Mo atoms that are connected to O atoms, these calculations lead to the number of oxidation states of +3.72(3), +3.82(3), +3.84(3), and +3.88(3) for Mo2, Mo3, Mo4, and Mo5, which are connected to seven atoms of Mo and to four atoms of O, respectively, and +2.75(4) and +2.80(4) for Mo6 and Mo7, which are connected to four atoms of Mo and five atoms of O. From these values, we could estimate the metallic electron count per Mo_{19} cluster as 68.5(5) e^-, which is a little larger that the value of 67.8 e^- based on the stoichiometry. In $Pr_4Mo_9O_{18}$[23] and $Mg_{4.5}Pr_{79.5}Mo_{126}O_{312}$,[32] which contain also Mo_{19} clusters but have other types of Mo clusters, the bond length−bond strength relationship developed by Brown and Wu yields values of 69.1(5) and 68.2(4) e_- per Mo_{19} cluster, respectively. Finally, it is interesting to note that for compositions ranging from about $Ca_7Pr_{10}Mo_{19}O_{46}$ to $Ca_4Pr_{13}Mo_{19}O_{46}$ for which single-phase powders are obtained, the number of electrons per Mo_{19} cluster range from 66 to 69 e^-.

3.3. Magnetic and Electrical Resistivity Properties. Figure 8 shows the temperature dependence of the inverse susceptibility below 300 K for $Ca_4Pr_{13}Mo_{19}O_{46}$, $Ca_5Pr_{12}Mo_{19}O_{46}$, $Ca_6Pr_{11}Mo_{19}O_{46}$, and $Ca_7Pr_{10}Mo_{19}O_{46}$. The

(33) Brown, I. D.; Wu, K. K. *Acta Crystallogr.* **1976**, *B32*, 1957.

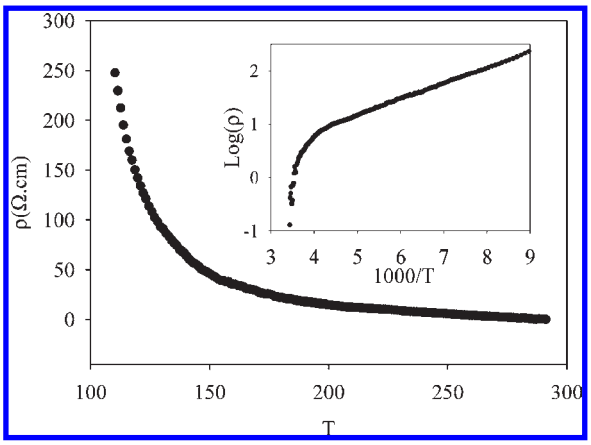

Figure 9. Temperature dependence of the electrical resistivity of a crystal of $Ca_{\sim 5}Pr_{\sim 12}Mo_{19}O_{46}$. Inset: Arrhenius plot.

magnetic susceptibilities of the latter four compounds follow the Curie−Weiss behavior over the 4.2−300 K temperature range. The susceptibility data were fitted to a modified Curie−Weiss law, $\chi = C/(T - \theta) + \chi_0$ in the 50−300 K temperature range. From the different fits, we could deduce effective moments μ_{eff} ranging from 3.56 and 3.62 μ_B, which are in good agreement with the value of 3.58 μ_B expected for trivalent Pr ions from Hund's rule.[34] No signature of magnetic ordering was found down to 4.2 K for the four compounds. On the other hand, contrary to what is observed for some Pr compounds, the characteristic behavior of a non-Kramers ion (i.e., a nonmagnetic singlet ground state) was not found in the compounds studied despite the low symmetry of the Pr^{3+} sites.[35]

Variable-temperature resistivity data for a single crystal of $Ca_{\sim 5}Pr_{\sim 12}Mo_{19}O_{46}$ in the temperature range 100−290 K are presented in Figure 9. $Ca_{\sim 5}Pr_{\sim 12}Mo_{19}O_{46}$ presents a degenerated semiconducting behavior with a resistivity of 0.4 Ω cm at room temperature and an activation energy of 0.8 eV at high temperature.

Supporting Information Available: Powder X-ray diffraction pattern of $Ca_5Pr_{12}Mo_{19}O_{46}$. This material is available free of charge via the Internet at http://pubs.acs.org.

(34) Van Vleck, J. H. *Electric and Magnetic Susceptibilities*; Oxford University Press: New York, 1932; p 243.

(35) (a) Kramers, H. A. *Proc. Amsterdam Acad.* **1930**, *33*, 959. (b) Bertaut, E. F. *Ann. Chim.* **1976**, *1*, 83.